PAPER • OPEN ACCESS

Newton flow of the Riemann zeta function: separatrices control the appearance of zeros

To cite this article: J W Neuberger *et al* 2014 *New J. Phys.* **16** 103023

View the article online for updates and enhancements.

Newton flow of the Riemann zeta function: separatrices control the appearance of zeros

J W Neuberger[1], C Feiler[2], H Maier[3] and W P Schleich[2,4]

[1] Department of Mathematics, University of North Texas, Denton, TX 76203-5017, USA
[2] Institute for Quantum Physics and Center for Integrated Quantum Science and Technology (IQST), Universität Ulm, D-89081 Ulm, Germany
[3] Institute for Number Theory and Probability Theory, Universität Ulm, D-89081 Ulm, Germany
[4] Texas A & M University Institute for Advanced Study (TIAS), Texas A & M University, Institute for Quantum Science and Engineering (IQSE), Texas A & M University, Department of Physics and Astronomy, Texas A & M University, College Station, TX 77843-4242, USA
E-mail: jwn@unt.edu, cornelia.feiler@uni-ulm.de, helmut.maier@uni-ulm.de and wolfgang.schleich@uni-ulm.de

Abstract

A great many phenomena in physics can be traced back to the zeros of a function or a functional. Eigenvalue or variational problems prevalent in classical as well as quantum mechanics are examples illustrating this statement. Continuous descent methods taken with respect to the proper metric are efficient ways to attack such problems. In particular, the continuous Newton method brings out the lines of constant phase of a complex-valued function. Although the patterns created by the Newton flow are reminiscent of the field lines of electrostatics and magnetostatics they cannot be realized in this way since in general they are not curl-free. We apply the continuous Newton method to the Riemann zeta function and discuss the emerging patterns emphasizing especially the structuring of the non-trivial zeros by the separatrices. This approach might open a new road toward the Riemann hypothesis.

S Online supplementary data available from stacks.iop.org/njp/16/103023/mmedia

Keywords: Riemann zeta function, continuous Newton method, Newton flow

1. Introduction

In ocean navigation, it has long been known [1] that traveling on a sphere with a constant oblique angle, relative to meridians, one is led eventually to one of the two poles. The resulting course of the ship is a spherical spiral which has been called a loxodromic curve (loxos+dromos from Greek, oblique+running). In complex analysis [2], following a line of constant phase of an analytic function one is led eventually to a zero or a pole of this function where several of these lines intersect. The continuous Newton method [3] takes advantage of this feature and represents an efficient algorithm to find the zeros of the function. In this article we apply this technique to the Riemann zeta function [5] and gain new insight into the overall structure of its zeros.

1.1. The Riemann zeta function in number theory and physics

The Riemann zeta function ζ is central to number theory [4], and in particular, in the distribution of the prime numbers p in the sea of natural numbers n. It is intimately connected to the function $\pi = \pi(n)$ which counts the number π of primes p below an integer n, and therefore increases by unity at p and is constant for a non-prime integer. Indeed, the analytical properties [5, 39] of ζ determine π. For example, the pole at $z = 0$ is responsible for the overall trend of π, and the non-trivial zeros provide us with the stair-case behavior of π and thereby distinguish the primes from the non-primes. However, even today, more than a hundred years after the discovery of this connection between the functions ζ and π expressed by the prime number theorem [6], the location of these zeros has not been proven mathematically. Notwithstanding the fact that by numerical techniques it has been shown to hold true for the first 10 billion of zeros [8, 9], the Riemann hypothesis [7] that all non-trivial zeros lie on an axis in the complex plane parallel to the imaginary axis with real part 1/2 is still an open mathematical question.

Nevertheless, the Riemann zeta function also plays an important role in physics. Indeed, it appears in many physical phenomena ranging from quantum chaos [10] via nuclear physics [11] to Bose–Einstein condensates [12]. From the wealth of articles we only highlight three prominent examples of the appearance of ζ in physics. For a comprehensive review of this topic we refer to [13].

The statistics of the non-trivial zeros of ζ is identical to the one of energy levels of a nucleus, or of the eigenvalues of an appropriate classically chaotic system [14]. Moreover, it has also been shown that the Riemann zeta function emerges in quantum mechanics when one considers an appropriately prepared wave packet moving in a potential with a logarithmic energy spectrum [15]. Finally the Mellin transformation which is at the basis of the Riemann zeta function can be generalized [16] to a quantum Mellin transformation using the inverted harmonic oscillator.

Indeed, the last two connections have given rise to suggestions for the experimental implementation of the Riemann zeta function. With the help of a logarithmic analogue of the Jaynes–Cummings model and appropriate joint measurements we [17, 18] can obtain ζ in the critical strip. In this scheme the entanglement of the quantum systems plays a crucial role. On the other hand, the Mellin transform allows a representation of ζ in the far field of a radiation

field described by classical electrodynamics. This technique has already been realized by van der Pol [19] in 1947 and has been refined recently in [20].

1.2. Lines of constant phase and steepest descent

Contour plots are a popular and efficient technique to visualize complex functions. However, such diagrams reflect only part of the information since they bring out only lines where the amplitude, that is the absolute value, of the function remains constant; plots of lines along which the phase remains constant, which constitutes the complementary information, are extremely rare. It is the continuous Newton method [3] which provides us with these lines.

The continuous Newton method is a steepest descent method [21] to locate the zeros of a complex function. It has found wide applications in many different physical situations due to the fact that many phenomena in physics are governed by partial differential equations the solutions of which can be found by casting the problem into one seeking the minimum of a function. The Tricomi partial differential equation [22] which is a simple model for transonic flow, or the Gross–Pitaevskii equation which governs superconductivity [23], describes the phase transition of a laser [24], and rules the macroscopic wave function of a Bose–Einstein condensate [25, 26] are only two of many such examples from the class of problems converted into a search of zeros.

The efficiency of the continuous Newton method results from the gradient being taken with respect to a well-chosen metric. Such generalized gradients, so-called Sobolev gradients [27] lead not only to substantial advantages, both numerically and conceptually, but also provide us with more insight into the underlying physics of the considered phenomena. Moreover, these techniques are useful in simplifying rather complex and lengthy proofs of mathematical theorems such as the Nash–Moser theorem [28].

1.3. Relation to other work

Besides the contour reliefs of many special functions, the classic book by Jahnke and Emde [29] displays already in its first edition of 1933 several curves in the complex plane where the Riemann zeta function is real and thus its phase vanishes.

Curves where ζ assumes real values have been studied in more detail in the Doktorarbeit by Utzinger [30] in 1934 and are at the very heart of an equivalent formulation of the Riemann hypothesis put forward by Speiser [31] in the same year. Based on the topology of the lines of vanishing imaginary part of ζ he claims that all non-trivial zeros of the first derivative ζ' of ζ are located to the right of the critical line. Needless to say, there are also zeros of ζ' along the negative real axis situated between each pair of trivial zeros of ζ. Since they can be understood analytically Speiser refers to them as the trivial zeros of ζ'.

The work closest to ours is [32] which analyzes the curves in the complex plane where ζ is purely real or purely imaginary. The crossing of these lines defines the zeros of ζ. Since the emerging picture resembles the skeleton of a body under an x-ray this work carries the suggestive title 'x-ray of Riemann zeta function'. Motivated by this analogy we refer to the lines with Im $\zeta = 0$ as 'bones'.

It is interesting to compare and contrast our approach to the above mentioned ones. Throughout our article we focus exclusively on the lines of constant phase of ζ brought to light by the corresponding Newton flow. The resulting flow pattern shows that there are special lines,

the separatrices, which define the basins of attraction given by the zeros of ζ. The separatrices act like 'continental divides' for the flow.

Separatrices are lines of constant phase that pass through the zeros of the derivative ζ' of ζ. Since the phase of the separatrix is determined by the phase of ζ at the point where ζ' vanishes, the separatrices are in general not the bones shown in the x-ray [32].

We conclude by mentioning that [33] investigates the phase of the Riemann zeta function with the help of an Argand diagram. In contrast, we show the full lines of constant phase in the complex plane. Moreover, in [34] the flow of ζ is analyzed in great detail. However, we calculate the flow of the reciprocal of the logarithmic derivative, that is, the Newton quotient of ζ.

1.4. Outline of our article

Our article is organized as follows: in section 2 we first briefly review the continuous Newton method and show that the Newton quotient is the gradient with respect to the Riemannian metric given by the first derivative of the function. We then dedicate section 3 to a discussion of several examples of complex-valued functions visualizing the continuous Newton method. Here we illustrate especially the role of separatrices and emphasize their importance for the location of the zeros. We devote section 4 to an application of the continuous Newton method to the Riemann zeta function. In the conclusions of section 5 we summarize our main results.

In appendix A we identify the Newton quotient as the gradient with respect to the Riemannian geometry imposed by the complex function F. We then show in appendix B that in general there is no direct connection between electric and magnetic field lines. Finally, appendix C examines the origin of separatrices in the Newton flow and appendix D gives a short description how to generate the pictures of the Newton flow.

2. Continuous Newton method: essentials

In this section we briefly describe the continuous Newton method of finding zeros of a function by following the lines of constant phase. Moreover, we make contact with continuous descent methods.

2.1. Lines of constant phase terminate in a zero

We consider a function $F : \mathbb{C} \to \mathbb{C}$ which has a continuous derivative in an open set G containing a point z_0 such that $F'(z) \neq 0$ for all $z \in G$. We define a flow by the solution z of the differential equation

$$\dot{z}(t) = -\frac{F(z(t))}{F'(z(t))} \tag{1}$$

for all t in the interval $[0, b)$ with $b > 0$ and subjected to the initial condition $z(0) \equiv z_0$.

This equation which involves on the right-hand side the inverse of the logarithmic derivative of F, that is, the Newton quotient, implies

$$F'(z(t))\, \dot{z}(t) = -F(z(t)).$$

Hence, for $t \in [0, b]$ the derivative of the composition reads

$$(F(\dot{z}))(t) = -F(z(t))$$

which upon integration yields

$$F(z(t)) = F(z_0) \, e^{-t}. \tag{2}$$

This solution shows that for $b = \infty$, $F(z(t))$ decays exponentially to zero, that is,

$$\lim_{t \to \infty} F(z(t)) = 0$$

provided that $\lim_{t \to \infty} z(t)$ exists.

Granted that $F'(z_0) \neq 0$, F is invertible in some neighborhood of z_0, the trajectory is given there by

$$z(t) = F^{-1}\big(F(z_0) \, e^{-t}\big). \tag{3}$$

A key observation from (2) is that the phase of $F(z(t))$ is fixed by $F(z_0)$ for the whole trajectory. These Newton trajectories are such that the phase remains constant on a trajectory. Hence, the trajectories are lines of constant phase. A consequence of this property is that on a Newton trajectory, the real part of $F(z(t))$ is a constant times the imaginary part.

The totality of Newton trajectories forms the Newton flow and (2) gives it a sense of direction. Indeed, the trajectories always go from the initial condition to a zero of the function. This feature is built into the differential equation (1). Here the minus sign is a mere convention. If we would have chosen the plus instead of the minus sign the field lines would have still been the same but the direction would have been inverted.

2.2. Newton flow is steepest descent in a special metric

Along its contour lines a function is constant and the gradient which is orthogonal to them points at the steepest descent. We now motivate using heuristic arguments that the continuous Newton method is a steepest descent method, however with respect to a different metric.

Throughout this section we restrict ourselves to real-valued functions $\boldsymbol{F}(\boldsymbol{r})$ in three dimensions with arguments $\boldsymbol{r}$ in two space dimensions. For a more rigorous treatment including complex functions we refer to appendix A.

We consider the function

$$\phi(\boldsymbol{r}) \equiv \frac{1}{2} |\boldsymbol{F}(\boldsymbol{r})|^2$$

and determine the largest directional derivative, that is, we find the direction in which the gradient of ϕ is largest. The familiar approach evaluates the derivative of ϕ at $\boldsymbol{r}$ in the direction of $\boldsymbol{h}$ as

$$[(\boldsymbol{h} \cdot \nabla)\phi](\boldsymbol{r}) = [(\boldsymbol{h} \cdot \nabla)\boldsymbol{F}](\boldsymbol{r}) \cdot \boldsymbol{F}(\boldsymbol{r}), \tag{4}$$

where the dots indicate the familiar scalar product in two and three dimensions.

According to the Riesz representation theorem [35] a linear real-valued function can always be represented by any scalar product of two elements of the domain of this function. Hence, we can replace the scalar product in the directional derivative of ϕ given by (4) by the scalar product $(\boldsymbol{h} \cdot \boldsymbol{g})_{\mathrm{S}}$, where $\boldsymbol{g}$ will be chosen in a way that is convenient for the problem at hand. This additional freedom is made possible by the fact that we have introduced a new scalar

product indicated by the subscript S which is different from the one in two and three dimensions denoted solely by a dot.

Many different choices of a scalar product offer themselves. However, one is well-suited for the problem of finding a gradient with fastest descent. It is defined in terms of derivatives of $\boldsymbol{F}$ and reads

$$(\boldsymbol{h} \cdot \boldsymbol{g})_S \equiv [(\boldsymbol{h} \cdot \nabla)\boldsymbol{F}](\boldsymbol{r}) \cdot [(\boldsymbol{g} \cdot \nabla)\boldsymbol{F}](\boldsymbol{r}). \tag{5}$$

When we compare (4) and (5) and assume that the inverse $\boldsymbol{F}'^{-1}$ of the first derivative $\boldsymbol{F}'$ of $\boldsymbol{F}$ exists we immediately obtain the identity

$$[(\boldsymbol{g} \cdot \nabla)\boldsymbol{F}](\boldsymbol{r}) = \boldsymbol{F}(\boldsymbol{r}),$$

which implies the Newton quotient

$$\boldsymbol{g} = \boldsymbol{F}'^{-1}\boldsymbol{F}.$$

Hence, the continuous Newton method uses a Riemannian geometry whereas the gradient for ordinary continuous steepest descent is taken with respect to the ordinary Euclidean metric. From the theory of Sobolev gradients [21], there are many possible gradients in between, and issues such as numerical efficiency finally make the decisive choice.

3. Building blocks of continuous Newton method

We now illustrate the continuous Newton method for several examples of complex functions F. These cases form the building blocks for more complicated functions and will reemerge in section 4 when we apply this technique to the Riemann zeta function.

3.1. Sinks and sources

We start the discussion by considering a simple zero, a simple pole and the Möbius transformation to illustrate the origin of the sinks and sources of the Newton flow. The resulting patterns are reminiscent of electric or magnetic field lines. It is therefore intriguing to think of the lines of constant phase of a complex function as being generated by an appropriate arrangement of electric charges or magnetic dipoles, or more generally, complex functions being visualized by electro- or magnetostatics.

This analogy might not even be that far-fetched since properties of complex analysis [2] and, in particular, the Cauchy–Riemann differential equations are frequently used to solve boundary value problems in electrostatics [36]. However, the example of the Möbius function shows that there is no one-to-one correspondence between the field lines in electricity and the ones in the Newton flow of complex functions.

3.1.1. Simple zero.   We start our discussion with the linear function

$$F_l(z) \equiv z \tag{6}$$

which according to (2) leads to the trajectories

$$z(t) = z(0)e^{-t} . \tag{7}$$

Needless to say, we could have also integrated the equation

$$\dot{z} = -z \tag{8}$$

defining the Newton flow for F_l given by (6) directly to find the trajectory (7).

Each trajectory approaches the origin $z = 0$ of the complex plane which is the zero of F_l. Hence, a simple zero attracts the Newton flow and serves for it as a sink.

It is interesting to analyze this approach toward the origin in more detail. Indeed, the trajectories tend toward $z = 0$ in the radial direction with an angle fixed by the phase of the initial position $z(0)$. Therefore, the radial lines are the lines of constant phase of F_l. All lines, independent of the values of their phases meet and thereby terminate at the origin. In other words, a straight line through the origin really consists of two parts: the one with a positive real part corresponds to the phase β whereas the one with a negative real part has the phase $\beta + \pi$. This feature is a consequence of the sense of direction introduced by (1).

The trajectories of the Newton flow of F_l are reminiscent of the electric field lines of a negative charge. We recall that in electrostatics the electric field $\boldsymbol{E} = (E_x, E_y)$ is always curl-free, that is,

$$\mathrm{curl}\, \boldsymbol{E} \equiv \frac{\partial E_y}{\partial x} - \frac{\partial E_x}{\partial y} \equiv E_{y,x} - E_{x,y} = 0.$$

Here we have introduced a comma between the two subscripts to separate the components from the variables of differentiation.

The Newton field in the complex plane $z \equiv x + iy$ defined by

$$N_x \equiv -\mathrm{Re}\left(\frac{F_l}{F_l'}\right) = -x \qquad \text{and} \qquad N_y \equiv -\mathrm{Im}\left(\frac{F_l}{F_l'}\right) = -y$$

of the linear function F_l is curl-free, that is

$$\mathrm{curl}\, \boldsymbol{N} = N_{y,x} - N_{x,y} = 0.$$

3.1.2. Simple pole.　　Next we analyze a simple pole at the origin of the complex plane given by

$$F_p(z) \equiv \frac{1}{z}.$$

Since $F_p'(z) = -1/z^2$ the Newton flow equation (1) reads

$$\dot{z} = z$$

and differs from (8) representing a simple zero just by a sign. As a result, the Newton flow given by the trajectories

$$z(t) = z(0)e^t$$

points radially away from the pole at $z = 0$. We can therefore consider the pole as a source of the trajectories, very much in the spirit of a positive charge in electrostatics. Again, the Newton field is curl-free.

3.1.3. Simple zero plus simple pole.　　So far the patterns formed by the Newton flow have been curl-free. However, this feature is not true for an arbitrary function F as we show in appendix B. This fact stands out most clearly for the Möbius transformation
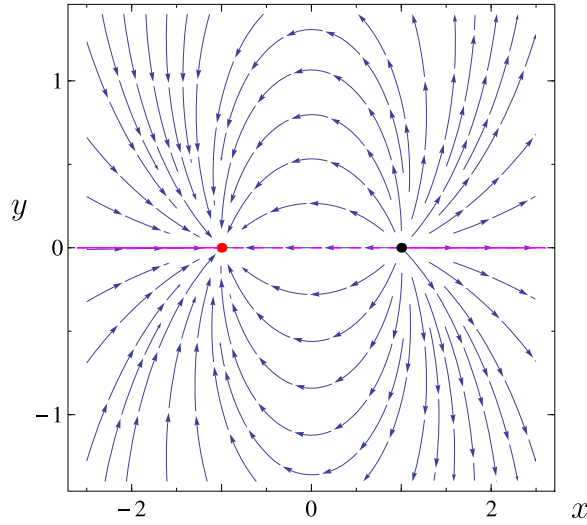
Figure 1. The Newton flow (10) for the Möbius transformation F_{M} defined by (9) and represented in the complex plane $z \equiv x + iy$ is reminiscent of the field lines of an electric dipole. The simple pole at $z = 1$ (black dot) serves as a source of the Newton trajectories. The simple zero at $z = -1$ (red dot) is the sink. Despite this close analogy, the Newton flow is not curl-free as shown in (11). Moreover, F_{M} is real only along the real axis with negative values on the dashed, and positive values on the solid violet curves, respectively.

$$F_{\mathrm{M}}(z) \equiv \frac{z + 1}{z - 1} \tag{9}$$

which displays a simple zero at $z_0 = -1$ and a simple pole at $z_{\mathrm{p}} = +1$. These points serve as the sink and the source of the Newton flow of F_{M} represented in the complex plane $z \equiv x + iy$ in figure 1.

Throughout the article red and black dots denote zeros and poles, respectively. Blue lines represent the Newton flow, that is, lines of constant phase of the function at hand. By virtue of (1) the flow lines have a sense of direction as indicated by the arrows.

Moreover, we have marked in violet the only line where the Möbius function is real. The dashing indicates negative values of F_{M}.

The pattern in figure 1 is reminiscent of the field lines of an electric dipole. However, in contrast to the electric field the Newton flow is not curl-free. Indeed, the first derivative

$$F_{\mathrm{M}}'(z) = -\frac{2}{(z - 1)^2}$$

of F_{M} (9) and the Newton flow defined by

$$\dot{z} = -\frac{F_{\mathrm{M}}(z)}{F_{\mathrm{M}}'(z)} = \frac{1}{2}\left(z^2 - 1\right) \tag{10}$$
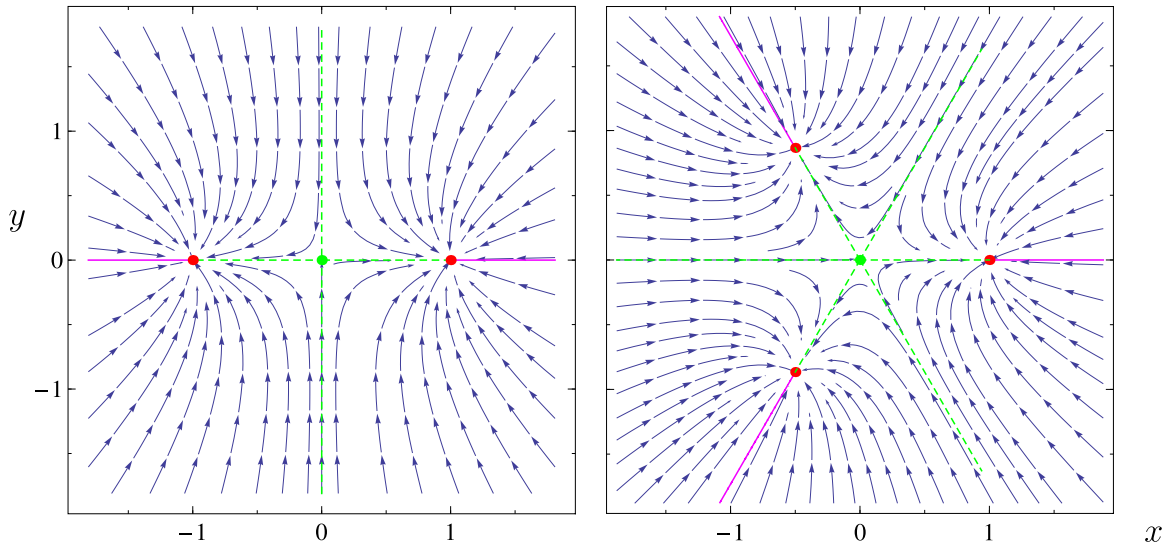
Figure 2. Newton flow lines in the complex plane $z \equiv x + \mathrm{i}y$ for the functions F_{d} (left) or F_{t} (right) defined by (12) identify the simple zeros (red dots) at $z = \pm 1$ or at $z = \mathrm{e}^{2\pi \mathrm{i}k/3}$ with $k = 1$, 2 and 3, respectively. We emphasize the special role of the origin (green dot), where two or three incoming flow lines (green dashed) meet. When one of these trajectories hits the origin, there is a choice in how to reach the zeros, illustrating the loss of forward uniqueness for (1). Along these separatrices the values of F_{d} and F_{t} are negative, whereas the positive values lie on the solid violet lines.

leads us to the components

$$N_x \equiv -\operatorname{Re}\left(\frac{F_{\mathrm{M}}}{F_{\mathrm{M}}'}\right) = \frac{1}{2}\left(x^2 - y^2 - 1\right) \quad \text{and} \quad N_y \equiv -\operatorname{Im}\left(\frac{F_{\mathrm{M}}}{F_{\mathrm{M}}'}\right) = xy$$

and we find

$$\operatorname{curl} \boldsymbol{N} = N_{y,x} - N_{x,y} = 2y. \tag{11}$$

Hence, the curl is vanishing only along the real axis. It is only there that the Newton field is curl-free.

3.2. Separatrices as continental divides of the flows

Next we show that a vanishing first derivative of F gives rise to lines in the complex plane which control the Newton flow. In four examples we illustrate these separatrices, and compare and contrast them with the lines where the functions are real. By studying the Newton flows of the asymptotic expansions of the Riemann zeta function ζ for arguments with large positive, or large negative real parts we lay the groundwork for our corresponding analysis of ζ presented in section 4.

3.2.1. Vanishing derivative as origin of separatrices.
An additional ingredient of the Newton flow emerges from the functions

$$F_{\mathrm{d}}(z) \equiv z^2 - 1 \qquad \text{and} \qquad F_{\mathrm{t}}(z) \equiv z^3 - 1 \tag{12}$$

which in contrast to the other examples either contain two or three zeros located at $z = \pm 1$ or at $z = e^{2\pi ik/3}$ with $k = 1$, 2 and 3, respectively.

In figure 2 we show the Newton flow of both functions. We note three characteristic features: (i) the zeros represent basins of attractions for the trajectories, (ii) lines in the complex plane separate these domains, and (iii) the origin seems to repel the trajectories.

In order to analyze each of these properties in more detail we now have a closer look at the Newton flow

$$\dot{z} = -\frac{z}{2} - \frac{1}{2z} \tag{13}$$

of F_d and note that the Newton trajectories

$$z(t) = \pm \sqrt{\left[z^2(0) - 1\right] e^{-t} + 1} \tag{14}$$

following from (3) approach the zeros for $t \rightarrow \infty$ as expected.

However, we also draw attention to the different signs in (14) in front of the square root. They result from inverting the function F_d and the trajectories are the mirror images of each other with respect to the real and imaginary axis.

This example also points out another important feature of Newton trajectories. At least for polynomials, but from computational evidence much more generally, when the function F has two or more zeros the complex plane is divided in such a way that each point in an individual domain leads to the same zero. The domains are separated from each other by lines in the complex plane. In the case of F_d these separatrices are the imaginary axis and parts of the real axis as we shall show now.

For this purpose we consider as an initial condition a position $z(0)$ on the imaginary axis, that is, $z(0) = i y_0$. In this case the trajectory following from (14) reads

$$z(t) = \pm \sqrt{1 - \left(1 + y_0^2\right) e^{-t}}. \tag{15}$$

Since for $0 \leqslant t < t_0 \equiv \ln\left(1 + y_0^2\right)$ the argument of the square root is negative, we first follow the imaginary axis and approach the origin which we reach at t_0. For $t_0 < t$ the argument of the square root is positive and we now move along the real axis toward one of the two zeros. Indeed, due to the plus and minus signs in (15) we have two choices: we can either go to the right and follow the positive real axis toward the zero $z = +1$, or we can move on the negative real axis toward $z = -1$. In both cases the Newton trajectories terminate at the respective zero.

The bifurcation of the trajectory is a consequence of the vanishing of the first derivative

$$F_d' = 2z$$

of F_d at the origin which manifests itself in a non-uniqueness of the forward solution as shown in appendix C. In figure 2 and throughout this article we indicate the points where the first derivative of a function vanishes by green dots and the resulting separatrices by green lines.

In this context it is interesting to note that [37] contains a chapter on semigroups for which the underlying trajectories do not have forward uniqueness. These include the semigroups generated by Newton flows for complex polynomials and likely the one corresponding to the Newton flow for the Riemann zeta function ζ. However, this question of the semigroup of ζ goes beyond the scope of the present paper.
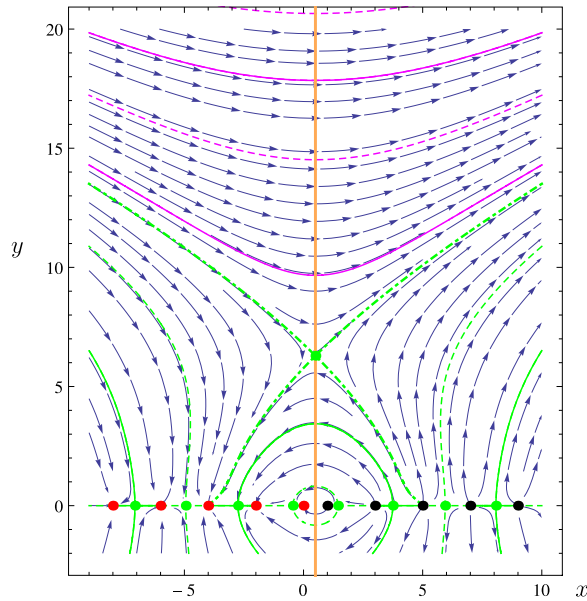
Figure 3. Newton flow lines of the function χ defined by (16) in the complex plane with positive imaginary part. On the separatrices (dot–dashed green lines) through the 'non-trivial' zero of χ' at $z \cong 0.5 + i\, 6.23$ the phase of χ is approximately $\pi/4$. These non-trivial separatrices divide the Newton flow into four domains: the flow lines which (i) come from $-\infty$ and end in a zero at $z_0 = -2k - 4$ with $k = 0, 1, 2,...,$ (ii) start at a pole $z_p = 2k + 5$ and approach $+\infty$, (iii) go from the pole $z_p = 1$ into the zero at $z_0 = 0$, from $z_p = 3$ into $z_0 = -2$, or from $z_p = 5$ into $z_0 = -4$, and (iv) reach from minus to plus infinity. In the domains (i), (ii) and (iii) the values of χ on the separatrices are negative (dashed green lines) or positive (solid green lines) in an alternating sequence. In region (iv) we find lines where χ is positive (solid violet) or negative (dashed violet), but these lines are not separatrices. The orange line marks the critical axis $x = 1/2$.

We now turn to the function F_{t} for which not only the first derivative F_{t}' but also the second derivative F_{t}'' vanishes at the origin. This feature produces three incoming and three outgoing separatrices as shown on the right of figure 2. Hence, the number of incoming and outgoing separatrices depends on the order of the first non-vanishing derivative at this point as demonstrated in appendix C.

Due to the fact that $F_{\mathrm{d}}(0) = -1$ and $F_{\mathrm{t}}(0) = -1$ the separatrices in these examples are the lines where the functions are negative indicated in figure 2 by the dashed green curves. Along the solid violet lines the functions are positive.

3.2.2. Complex phases. The function

$$\chi(z) \equiv \frac{\pi^{z - \frac{1}{2}}\, \Gamma\left((1 - z)/2\right)}{\Gamma(z/2)} \tag{16}$$

with the gamma function $\Gamma = \Gamma(z)$ plays an important role in the functional equation of the Riemann zeta function and is therefore central to our analysis in section 4.

Due to the poles of $\Gamma(z/2)$ in the denominator χ has zeros at the origin, and at the negative even integers, whereas the poles determined by the numerator are located at the positive odd integers as shown by the Newton flow in figure 3. Apart from the 'trivial' zeros of the derivative
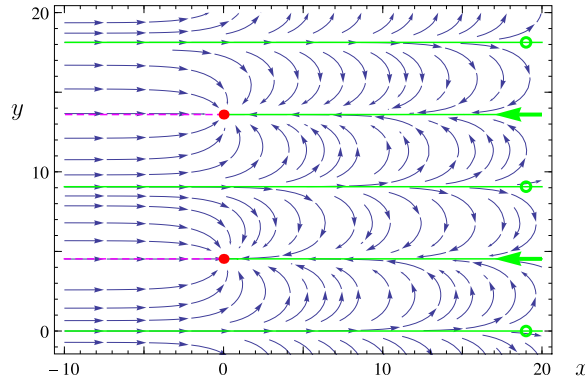
Figure 4. The Newton flow of the function F_e defined by (17) originates from $-\infty$ and either goes directly into the zeros (red dots) located at $z = \pm\, i\pi\,(2k + 1)/\ln 2$ with $k \in \mathbb{N}$, or passes them and turns around to finally get back to them. However, the separatrices between the zeros are straight lines which extend from $-\infty$ to $+\infty$ and the zeros of the derivative F_e', indicated by the green circles, are located at $+\infty$ with the imaginary parts $y = \pm\,\pi\,2k/\ln 2$. Since at these points $F_e = 1$, the function F_e is positive along these curves (solid green lines). The separatrices which tend toward the zeros of F_e, marked by green arrows, are the only ones starting at $+\infty$. The fact that F_e is also positive along these lines indicates that they are connected to the zeros of F_e' although their imaginary part is the same as the one of the zeros of F_e. The dashed violet lines mark the curves where F_e is negative.

χ' which are located on the real axis between two adjacent zeros and between two poles, there are two 'non-trivial' zeros of χ' on the critical line $x = 1/2$ (orange) with imaginary part $y \cong \pm 6.23$. In each of them two separatrices cross.

The dot–dashed green lines in figure 3 indicate the 'non-trivial' separatrices in the part of the complex plane with positive imaginary part where the phase of χ is approximately $\pi/4$. They divide the Newton flow into four domains: (i) On the left of the non-trivial zero, the flow lines come from $-\infty$ and terminate in the trivial zeros of χ with $z \leqslant -4$, whereas (ii) on the right the flow lines start at the poles with $z \geqslant 5$ and end at $+\infty$. (iii) Below the non-trivial zero of χ' we find flow lines emerging from the poles at $z_p = 1$, $z_p = 3$ or $z_p = 5$ and terminating in the zeros $z_0 = 0$, $z_0 = -2$ or $z_0 = -4$, respectively. (iv) Above the two separatrices the flow lines cross the complex plane from $-\infty$ to $+\infty$.

Since the values of χ are real on the real axis but with alternating signs for neighboring trivial zeros of χ', the function χ is real with alternating signs on the separatrices in the regions (i), (ii) and (iii). The separatrices in the third domain connect the trivial zero of χ' at $z' \cong 3.75$ with $z' \cong -2.75$, as well as $z' \cong 1.45$ with $z' \cong -0.45$ and enclose the Newton flow between the poles and zeros. In the fourth region, we find of course flow lines where χ is positive (solid violet) or negative (dashed violet) but which do not represent separatrices.

It remains to be mentioned that we have neglected on purpose to draw the non-trivial separatrices in the complex plane with negative imaginary part since there the phase of χ is approximately $-\pi/4$ due to the property $\arg[\chi(x - iy)] = -\arg[\chi(x + iy)]$.

3.2.3. Influence of infinity. We now show that separatrices may also occur if the zeros of the derivative of the function are located at infinity. Indeed, the function

$$F_e(z) \equiv 1 + e^{-z \ln 2} \tag{17}$$

possesses besides the zeros at $\pm i\pi (2k + 1)/\ln 2$ with $k \in \mathbb{N}$, zeros of F_e' for $x \to \infty$ and $y = \pm i\pi 2k/\ln 2$, depicted in figure 4 by the green circles.

For the function F_e the lines separating the flows are parallel to the real axis and we can identify two different types: (i) The ones coming from $-\infty$ go straight into the corresponding zero of F_e' at $+\infty$. (ii) The others start at $+\infty$ but with an imaginary part which is identical to the one of the zero of F_e they are ending in.

The fact that F_e is positive on both types of these lines shows that the ones emerging from $+\infty$ are actually the continuations of the ones from $-\infty$ which approach the zeros of F_e', where $F_e = 1$.

We emphasize that this feature stands out most clearly when we represent the complex plane by the Riemann sphere and consider the Newton flow of the Riemann zeta function in this representation. The separatrices which correspond to the ones of F_e emerge from the north pole to the left, circumvent a non-trivial zero of ζ and return to the north pole from the right only to reappear again to the right. For a more detailed discussion we refer to [38].

To stress that the lines of type (ii) are the only ones which really come from $+\infty$ we mark them by green arrows. All other flow lines start at $-\infty$.

3.2.4. Forward uniqueness exists at a double zero. In the preceding subsection we have shown that the points z where the first derivative of F vanishes play a crucial role for the Newton flow since here the separatrices split up. However, such a bifurcation does not occur when also F vanishes at this point.

In order to bring out this fact most clearly, we consider the function

$$F_2(z) \equiv z^2$$

which gives rise to the Newton flow

$$\dot{z} = -\frac{1}{2} z$$

and the trajectory

$$z(t) = z(0) e^{-t/2}.$$

As a result, a double zero is also a sink despite the fact that F' vanishes. However, we approach it with a speed which is half of that of a simple zero.

4. Newton flow of Riemann zeta function

In the present section we apply the continuous Newton method to the Riemann zeta function ζ. For the sake of completeness we first summarize important features of ζ and then discuss the emerging patterns using the elementary building blocks outlined in the preceding section. In particular, we focus on the grouping of the non-trivial zeros within their individual basins of attraction, and the appearance of separatrices fencing off the individual groups of zeros from each other. Moreover, we make contact with the 'bones' of the x-ray of ζ discussed in [32].

4.1. Riemann zeta function in a nutshell

For a complex argument $z \equiv x + iy$ with $1 < x$ the Riemann zeta function ζ follows from the Dirichlet sum

$$\zeta(z) = \sum_{n=1}^{\infty} \frac{1}{n^z}, \tag{18}$$

which in this part of the real axis is convergent.

Since for $z = 1$ the Dirichlet sum reduces to the harmonic sum which is divergent, we find a simple pole of ζ at $z = 1$.

In his seminal article [7] Riemann was able to provide an analytical extension of ζ onto the domain of the complex plane left of $z = 1$ and today many such expressions exist [39]. In particular, the representation

$$\zeta(z) = \chi(z)\, \zeta(1 - z) \tag{19}$$

shows that at the negative even integers simple zeros of ζ appear due to the negative zeros of the function χ defined by (16) and shown in figure 3. At $z = 0$ the zero of χ is canceled by the pole of ζ at $z = 1$. Since the location of these zeros are known they are called 'trivial zeros'.

Moreover, it was shown [40] that the only real zeros of the derivative ζ' lie on the negative real axis, one between two adjacent trivial zeros of ζ. Hence, we call them 'trivial zeros of the derivative'.

More interesting are the so-called 'non-trivial' zeros of the zeta function. According to the Riemann hypothesis they all have real part 1/2 which is in complete analogy to the statement that ζ' has no non-real zeros for $x < 1/2$ [31, 40].

However, so far this conjecture has not been verified yet and is one of the one-million dollar questions of the Clay Mathematics Institute [41]. Needless to say, in the present paper we are not going to solve the Riemann hypothesis either but apply the continuous Newton method to study the lines of constant phase of ζ which bring out structures in the grouping of the non-trivial zeros.

4.2. Flow lines

In section 3 we have introduced the building blocks of the continuous Newton method. We now apply this technique to the Riemann zeta function. We start with the behavior of ζ for $x \to \pm\infty$, then analyze the neighborhood of the real axis and finally work our way up the critical axis where the non-trivial zeros are located.

4.2.1. Approximations for large real parts of the argument. For large positive real parts x the Riemann zeta function can be approximated by the function F_e defined by (17) which consists of the first two terms of the Dirichlet series (18), that is

$$\zeta(z) \cong 1 + e^{-z \ln 2} = F_e(z).$$

As a result, in the right picture of figure 5 the separatrices of ζ come from $x \to -\infty$ and end in the zeros of the derivative ζ', that is at $y = \pm\, \pi\, 2k/\ln 2$ and positive infinite x, marked by green circles. The green arrows indicate the only lines coming from $+\infty$ with imaginary parts $\pm\pi\,(2k + 1)/\ln 2$.
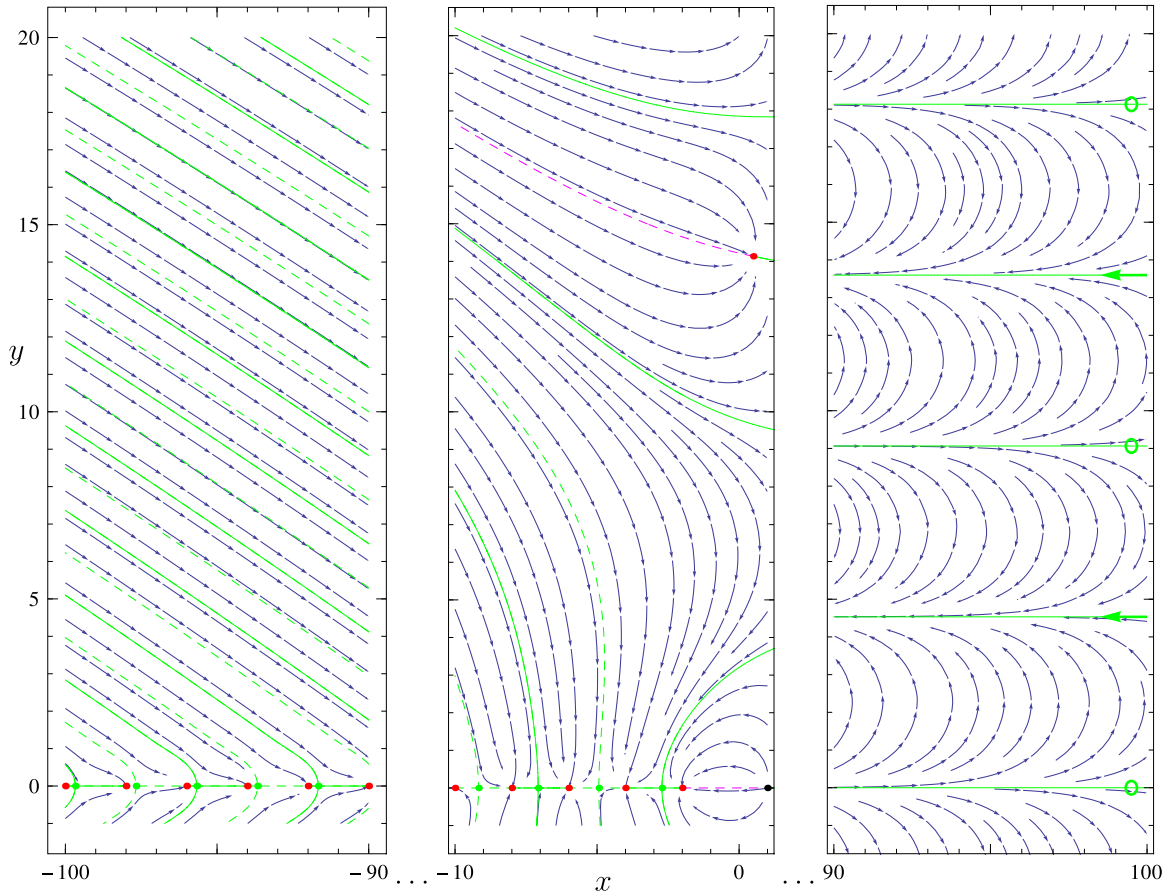
Figure 5. Newton flow of the Riemann zeta function in three different regions of the
complex plane. Since for $x \to -\infty$ we can approximate ζ by χ, and for $x \to +\infty$ by F_e,
the flow lines in the left and right pictures are similar to the ones of χ and F_e shown in
figures 3 and 4. Hence, in the right picture the separatrices (green lines) run parallel to
the real axis from left to right into the vanishing derivative ζ' at $x \to +\infty$ with
imaginary part $y = \pm\pi\, 2k/\ln 2$ (green circles) and continue from right to left at
imaginary parts $y = \pm\pi\,(2k+1)/\ln 2$ (green arrows). In contrast, we find in the
domain of the complex plane with large negative real parts separatrices along which ζ is
real but with alternating signs. They divide the complex plane such that the Newton
flow reaches the trivial zeros at $x = -2k$. The middle picture shows ζ for intermediate
negative values and in the critical strip which illuminates the connection between the
outside regions and is discussed in detail in the remainder of this subsection.

The left picture of figure 5 shows the Newton flow of ζ for $x \to -\infty$. In this domain we get
from the functional equation (19) the expression

$$\zeta(z) \cong \left(1 + e^{-(1-z)\ln 2}\right)\chi(z), \tag{20}$$

where we have approximated ζ on the right-hand side of (19) by the first two terms of the
Dirichlet series.

Hence, the behavior there is mainly given by the function χ which produces the trivial
zeros of ζ. Moreover, the trivial zeros of the derivative of ζ' located between two trivial zeros of
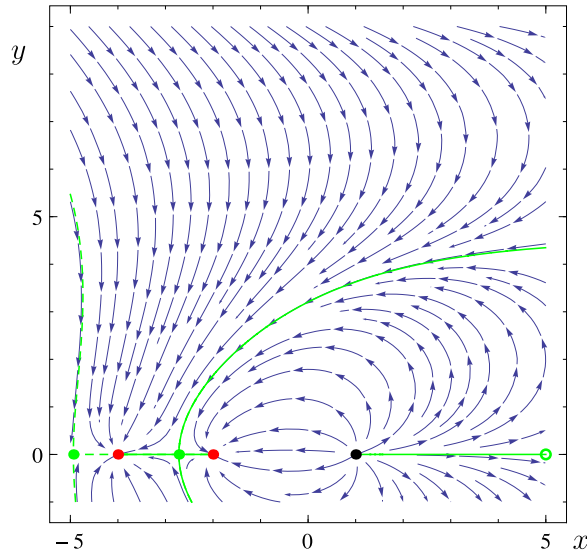
Figure 6. Newton flow lines for ζ in the neighborhood of the real axis show the source point at the simple pole $z = 1$ (black dot) and two sinks represented by the trivial zeros at $z = -2$ and $z = -4$ (red dots). The zeros of ζ' at $z' \cong -2.72$ and $z' \cong -4.938$ (green dots) are unstable equilibria for the Newton flow. Like χ in figure 3, ζ is real on the separatrices (green lines) in this region and negative (dashed green line) on the one left to the zero at $z = -4$ which starts at $-\infty$. Although, ζ is positive on the separatrix between -4 and -2 this separatrix now emerges from $+\infty + \mathrm{i}\, 3\pi/\ln 2$ due to the Dirichlet series. This influence also causes a tiny shift of the trivial zeros of ζ' to the right compared to the zeros of χ' at $z' \cong -2.75$ and $z' \cong -4.943$.

ζ are not identical to the trivial zeros of χ'. Indeed, they are slightly shifted to the right due to the influence of the remnant $\exp[-(1 - z)\ln 2]$ of the Dirichlet sum in (20).

Nevertheless, along the separatrices through these points ζ is real with alternating signs. These separatrices are displayed by solid or dashed lines for positive or negative values, respectively.

In the middle of figure 5 we depict the Newton flow of ζ for $-10 \leqslant x \leqslant 1$ which illustrates the connection between the asymptotic behaviors on the left and on the right. A detailed description of the structures in this intermediate domain follows in the remainder of this subsection. However, it is interesting to note that the zeros of the approximation of ζ given by (20) are located on the line $x = 1$, which defines the right border of the critical strip, whereas F_e has zeros on the left border $x = 0$. According to the Riemann hypothesis the non-trivial zeros of ζ are at $x = 1/2$.

4.2.2. Neighborhood of simple pole and trivial zeros.   In figure 6 we show the Newton flow in the neighborhood of the real axis around the origin of the complex plane. Here we display the behavior for positive imaginary parts up to $y = 9$ and focus on a small domain along the negative imaginary axis. However, we emphasize that the structure of the Newton flow of ζ is symmetric with respect to the real axis but the phase of ζ for negative imaginary parts has the complementary sign due to $\arg[\zeta(x - \mathrm{i}y)] = -\arg[\zeta(x + \mathrm{i}y)]$.

In this excerpt of the complex plane we include the simple pole of ζ at $z = 1$ and the first two trivial zeros at $z = -2$ and $z = -4$. The field lines emerge from the pole and converge
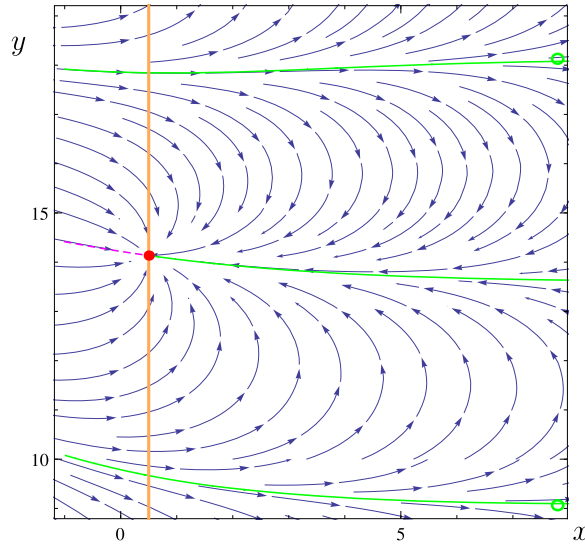
Figure 7. Newton flow lines for ζ in the neighborhood of the critical line (orange) and the first non-trivial zero at $z \cong 1/2 + \mathrm{i}\, 14.135$ (red dot). The green lines represent the separatrices of ζ. The upper and lower one cross the critical line from the left to the right ending at the zeros of the derivative ζ' with $x \to \infty$ at imaginary parts $y = (2\pi/\ln 2)$ and $y = (4\pi/\ln 2)$, respectively, indicated by the green circles. Hence, the values of ζ on these lines are real and positive. Along the middle separatrix which starts at $+\infty + \mathrm{i}\,(3\pi/\ln 2)$ and approaches the zero from the right ζ is also positive. This separatrix is connected by the zero to a line coming from the left, marked by the dashed violet line, where ζ is negative. In the domain of the complex plane displayed here the derivative of ζ does not vanish.

toward the first trivial zero in a way reminiscent of the Newton flow of the Möbius transformation shown in figure 1. However, in the case of ζ there is a slight asymmetry with respect to the center at -0.5 with more weight toward the source. This effect is caused by the influence of the Dirichlet series in the functional equation (19).

In the right half of the complex plane we have a separatrix starting at the pole which ends at the zero of ζ' at $+\infty$ indicated by the green circle. Here ζ is positive. Likewise on the separatrix into the zero of ζ' at $z' \cong -2.72$ which starts at $+\infty + \mathrm{i}\, 3\pi/\ln 2$ we find positive values for ζ.

In contrast, on the separatrix to the left of the trivial zero $z = -4$ through the trivial zero of ζ' at $z' \cong -2.72$ the values of ζ are negative. This separatrix is the one of χ which runs through $z' \cong -2.75$ but is shifted to the right due to the Dirichlet series in the functional equation (19).

4.2.3. Neighborhood of critical line. We now turn to analyze the Newton flow in the neighborhood of the critical line and the non-trivial zeros. In figure 7 we show the Newton flow around the first non-trivial zero at $z \cong 1/2 + \mathrm{i}\, 14.135$.

The upper green solid line partitions the flow going down to the first non-trivial zero from the one going up to the second one. Likewise, the lower green solid line separates the flow going up to the first non-trivial zero from the one going down to the real axis shown on the top of figure 6. Both come from the left and aim for the zeros of ζ' at $+\infty + \mathrm{i}\, 4\pi/\ln 2$ and $+\infty + \mathrm{i}\, 2\pi/\ln 2$, respectively. Hence, the values of ζ on these lines are positive.
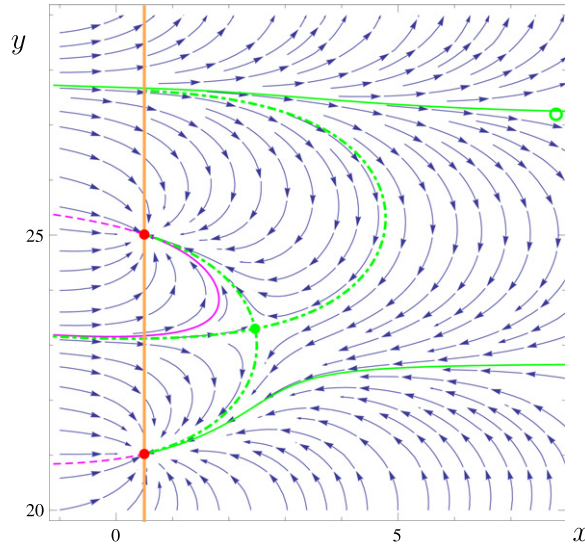
Figure 8. Newton flow lines for ζ in the neighborhood of the critical line (orange) and the second and third non-trivial zero (red dots). There is a zero of ζ' (green dot) between them which determines the dot–dashed green separatrix dividing the flow between the two zeros. On this line the argument of ζ is approximately $0.01\,\pi$ whereas on the other two separatrices (solid green lines) ζ is positive. The upper one divides the complex plane and ends at the zero of ζ' at $+\infty + \mathrm{i}\,6\pi/\ln 2$ while the lower one comes from $+\infty + \mathrm{i}\,5\pi/\ln 2$ and approaches the second non-trivial zero of ζ from the right. The violet curves indicate the other lines where ζ is positive (solid) or negative (dashed).

These two separatrices are reminiscent of the first two solid violet lines above the separatrix through the non-trivial zero of χ' shown in figure 3. However, we emphasize that not all positive real lines of χ which start at $-\infty$ are separatrices for the Riemann zeta function.

Nevertheless, we recognize that almost all field lines approach from the left and either converge directly toward the zero, or first pass it by going far to the right and then turn around to eventually also arrive at the zero. The only exception is the separatrix starting at $+\infty + \mathrm{i}\,3\pi/\ln 2$, indicated by the middle solid green line. It reaches the zero from the right.

We have to note here that the 'x-ray' [32] already studies the 'bones' of ζ, that is the lines where ζ is real and interprets all which reach from minus to plus infinity as a single entity. Yet, we emphasize that those which go through a non-trivial zero of ζ really consist of two parts: (i) the one approaching the zero from the right on which ζ is positive and (ii) the one coming from the left on which ζ is negative. In figure 7 we have indicated by the dashed violet curve the part (ii) of the 'bone' through the first non-trivial zero.

It would be interesting to see which consequences arise from this new interpretation of lines of this kind brought to light by the Newton flow when applied to the argumentation in [32]. However, we have to postpone a more detailed discussion of this question to a future publication.

In the domain of the complex plane shown in figure 7 there is no point, where ζ' vanishes. In contrast, the Newton flow depicted in figure 8 in the neighborhood of the next two non-trivial zeros clearly experiences the consequences of ζ' vanishing at $z' \cong 2.46 + \mathrm{i}\,23.4$. The flows coming from the right approach the two zeros above or below of this point of non-equilibrium. Likewise, the flow from the left splits up into two parts. The resulting separatrix on which the
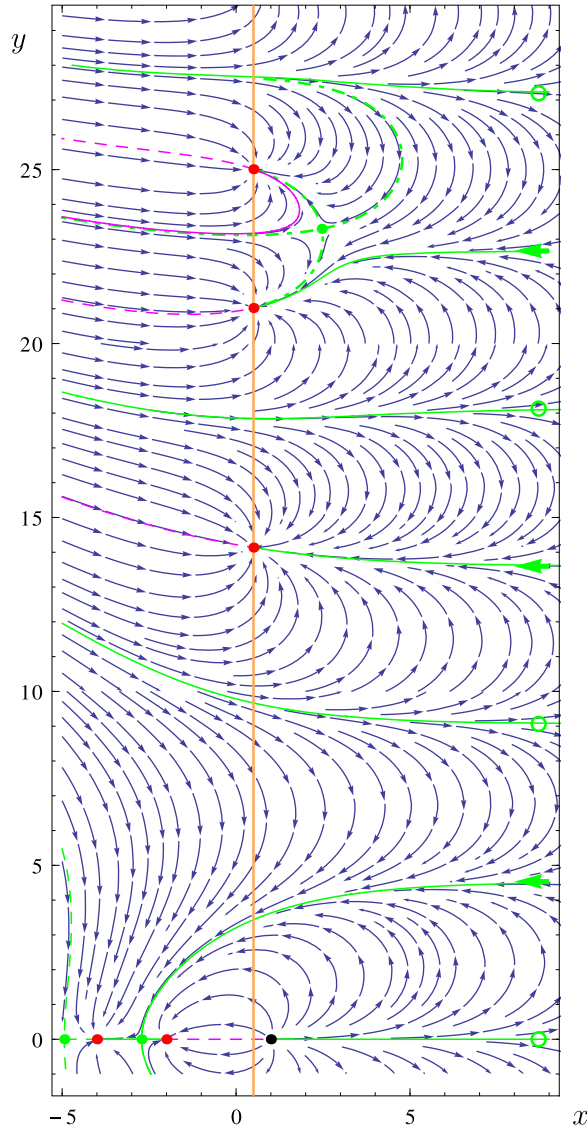
Figure 9. Newton flow lines for ζ along the real axis and the critical line (orange) on a larger scale combining figures 6–8. We recognize the pole at $z = 1$ (black dot), the first two trivial zeros and the first three non-trivial zeros (red dots), together with the trivial and the non-trivial zeros (green dots) of ζ'. The separatrices (green lines) cross the zeros of ζ' at plus infinity (green circles) and return as flow lines (green arrows) starting at $+\infty$. The phase of ζ along the separatrices is determined by the value of ζ at the zero of the derivative ζ' which they cross. Along the solid and dashed green lines, as well as along the violet curves ζ is real.

phase of ζ is approximately $0.01\,\pi$ is indicated by the dot-dashed green line. It explains the attraction of the lines where ζ is real (violet and green solid curve) to the zero of the derivative of ζ mentioned in [32].

In figure 9 we present an overview of the Newton flow of ζ for the domain $[-5, 9] \times [-1, 30]$ of the complex plane which summarizes the details contained in the previous pictures.

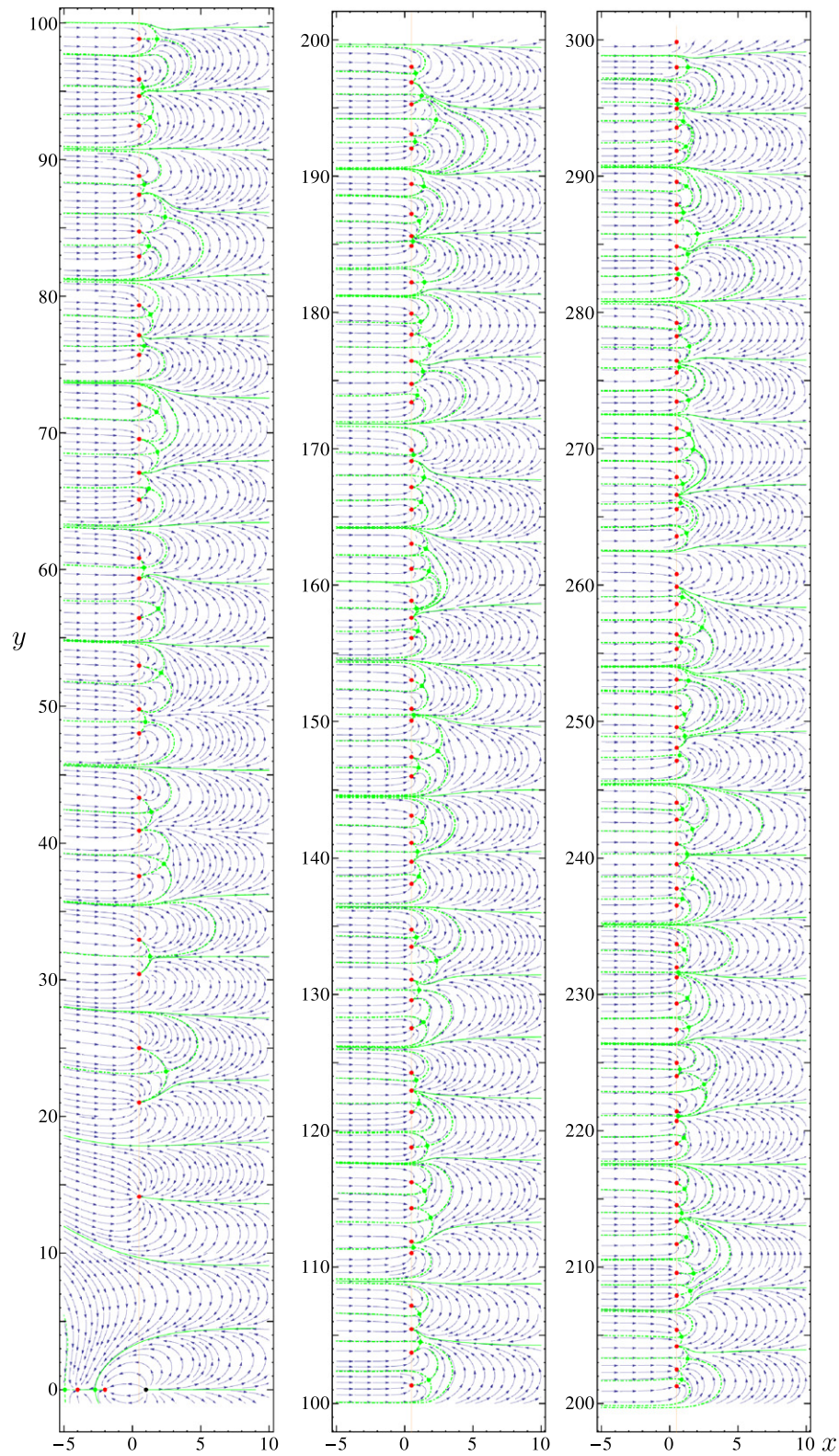**Figure 10.** Newton flow of ζ along the critical axis in the domain of $-1 \leqslant y \leqslant 300$ represented in three consecutive panels with increasing imaginary part. For an interactive and much expanded version of these figures see the supplementary data.

So far we have only shown small excerpts of the rich structure contained in the Newton flow of ζ. In the supplementary data we show a figure with a much larger domain of the complex plane accessible by scrolling up and down the imaginary axis. In order to give a flavor of this picture we display in figure 10 the first three consecutive parts of this scroll which bring out a structure of the grouping of the non-trivial zeros along the critical line. Indeed, it arises from the separatrices which pass the complex plane from minus to plus infinity along which ζ is positive. The non-trivial zeros of ζ in one of these groups are separated by separatrices through the zeros of ζ' where ζ is not real. There is always one zero of the derivative less than zeros of ζ.

The pictures also show that the real lines starting at minus infinity have alternating signs for increasing imaginary part and all negative lines (dashed violet) end directly at a zero of ζ without ever crossing the critical line.

4.3. More insights into ζ from the Newton flow

The present article is meant to be an appetizer for a more detailed application of the Newton flow to unravel the unique properties of the Riemann zeta function which is so prominent in physics. Many further developments come to mind. Here we only briefly mention three since a more elaborate discussion would go beyond the scope of our article.

4.3.1. Universality theorem. In 1975 Mikhailovitch Voronin [42] showed that any non-vanishing holomorphic function in a circle with radius less than 1/4 can be approximated by the Riemann zeta function somewhere in the strip defined by $1/2 \leqslant x \leqslant 1$. Indeed, figure 10 and especially the scroll version of it demonstrates that this domain of the complex plane is continuously changing as the imaginary part increases. It is therefore reasonable that there ζ can approximate every non-vanishing holomorphic function. However, a more detailed study of this visualization of the universality theorem is needed.

4.3.2. Appearance and disappearance of zeros. Another interesting application of the Newton flow emerges from the representation

$$\zeta(z) \equiv \frac{1}{2^{1-z} - 1} \sum_{n=1}^{\infty} \frac{(-1)^n}{n^z}$$

of ζ in the critical strip $0 < y < 1$ in terms of an alternating sum [39].

Here one might investigate how the locations of the zeros depend on the truncation parameter when we realize ζ by a finite rather than an infinite sum. The motion of the zeros in the complex plane as we take more terms and their appearance and disappearance might shine some light onto the Riemann hypothesis and the results of Turán [43] and Montgomery [44].

4.3.3. Riemann hypothesis. Newton flows may also offer a possible new approach to the Riemann hypothesis. Our figures indicate that in the critical strip the zeros are grouped in a natural way by roughly horizontal separatrices on which ζ is positive. The first group contains just one zero. The next two groups have two zeros each, and the later ones have three or more zeros, all separated by separatrices on which ζ assumes complex values.

Hence, the denial of the Riemann hypothesis would lead to a pair of zeros situated symmetrically about the critical line with an additional zero of the derivative separating the Newton flow into these zeros. The pattern of groups of zeros would likely be severely disturbed.

If the supposition of such a disturbance were to lead to a contradiction, the Riemann hypothesis might be established.

We do not express any particular expectation that such a program might be successfully completed, but the present work suggests a qualitative, topological approach to the Riemann hypothesis.

5. Conclusion

A wide class of partial differential equations arising in physics can be posed as zero-finding problems. Gradient continuous descent methods [21, 27] present a means for dealing with many of them, but it is becoming increasingly clear that in a given situation, a gradient taken with respect to a well-chosen metric provides substantial advantages, both numerically and theoretically. An understanding of the paths followed by the continuous descent often yields important information. An extensive discussion of Sobolev gradients reveals [21] how gradient choices impact issues in the study of partial differential equations.

In the present article we have applied a special example of a gradient continuous descent method, that is the continuous Newton method to several complex functions. Four results stand out most clearly: (i) The continuous Newton method is an effective tool to find the lines of constant phase of a complex-valued function F since the Newton quotient represents a gradient taken with respect to a natural Riemannian metric which naturally produces these lines. (ii) The sinks and sources of the Newton flow identify the zeros and poles of F, respectively. (iii) The flow lines from or into the individual poles or zeros are separated by separatrices which cross each other in the point where the derivative F' vanishes. (iv) The number of crossing separatrices is determined by the order of the first non-vanishing derivative.

The Newton flow of the Riemann zeta function formed by the lines of constant phase puts 'flesh' on the 'bones' visible in Arias-de-Reynas x-ray [32] which are the lines where ζ is real. However, throughout the article we have emphasized the importance of the separatrices rather than of the bones for the distribution of the zeros of ζ. Indeed, separatrices which are lines of constant phase that go through the zeros of the derivative ζ' represent 'continental divides' for the Newton flow and control in this way the appearance of the zeros.

We have identified two kinds of separatrices: (i) On the ones which run from minus to plus infinity where they cross a zero of ζ' and then continue from plus infinity to a non-trivial zero, ζ is positive. (ii) In contrast, on the separatrices through a non-trivial zero of ζ' in the neighborhood of the critical line, ζ is complex.

Indeed, the topology of the separatrices might open a new approach toward the longstanding question of the Riemann hypothesis. If there were to be a counter-example to the Riemann hypothesis, there would have to be a separatrix running between two very close zeros, on opposite sides of the critical line. Such a separatrix might have no legitimate way to go to the Edge of Infinity, thus providing a negation of a supposition that there are two such zeros.

Acknowledgements

Appendix A. Riemann–Sobolev–Newton (RSN)

In section 2.2 we have used heuristic arguments to motivate the fact that the Sobolev gradient associated with F and taken with respect to the natural Riemannian metric is the Newton quotient. In the present appendix we provide the mathematical foundation for this statement. In particular, we now deal with a complex-valued function F.

We begin with some comments on Riemannian geometry which is partially rooted in thoughts of Gauss. We suppose that n is a positive integer and F is a function from $\mathbb{C}^n \to \mathbb{C}^n$ which in an open subset G of $\mathbb{C}^n$ is such that the Jacobian derivative $F'(z)$ exists and has an inverse for all $z \in G$. Moreover, we denote the image of G under F by M.

For each $z \in G$ and $g, h \in \mathbb{C}^n$ there is a metric

$$\langle g, h \rangle_z \equiv \langle F'(z)g, F'(z)h \rangle \tag{A.1}$$

on $\mathbb{C}^n$ induced by the tangent space to M. Here $F'(z)g$ denotes the derivative of F in the direction of g at the point z and $\langle \cdot, \cdot \rangle$ is the standard inner product (dot product) on the complex n-dimensional space.

Given $z \in G$, the norm associated with the inner product in (A.1) is denoted by $\| \cdot \|_z$ whereas the standard norm in $\mathbb{C}^n$ is abbreviated simply by $\| \cdot \|$. For fixed $z \in \mathbb{C}^n$, the norm of a linear transformation $T : \mathbb{C}^n \to \mathbb{C}$ indicated by $| \cdot |$ is defined by

$$|T| \equiv \sup_{w \in \mathbb{C}^n, \, \|w\|_z = 1} |Tw| .$$

Next, we provide a geometric interpretation of this second inner product of the two elements $g, h \in \mathbb{C}^n$ which according to (A.1) is the standard inner product of the directional derivatives $F'(z)g$ and $F'(z)h$. Due to the explicit appearance of F' we get a variable metric, one which changes from point to point in M, as is common in Riemannian geometry.

We now turn to the second character S in the title RSN of this appendix and illustrate the notion [21] of a Sobolev gradient, that is, the gradient of a function with respect to a varying metric. There is no need to invoke the concept of Sobolev spaces here to which Sobolev gradients are usually applied but rather we use the following fact: The derivative $\phi'(z)h$ of the function

$$\phi(z) \equiv \frac{1}{2} \|F(z)\|^2$$

in the direction of $h \in \mathbb{C}^n$ at $z \in G$ is given by

$$\phi'(z)h = \frac{1}{2} \Big(\langle F'(z)h, F(z) \rangle + \langle F(z), F'(z)h \rangle \Big). \tag{A.2}$$

Now, fixing $z \in G$, we seek a gradient of ϕ at z, that is we seek a vector $h \in \mathbb{C}^n$ which maximizes the function

$$\Phi(h) \equiv \frac{|\phi'(z)h|}{\| h \|_z} \tag{A.3}$$

over all $h \in \mathbb{C}^n$ different from zero. We emphasize that this is only one of several equivalent definitions, but note that it gives the standard gradient for ϕ only when the norm $\| \cdot \|_z$ is the standard norm $\| \cdot \|$. In this case we get the usual list of partial derivatives for a gradient.

In order to solve this maximum problem we first provide an upper bound for Φ and then present the specific choice of h for which this bound is assumed. For this purpose we apply the

Cauchy–Schwartz inequality to the scalar products on the right-hand side of (A.2) which yields

$$|\phi'(z)h| \leqslant \| F(z) \| \, \| F'(z)h \|. \tag{A.4}$$

Moreover, we find from the definition (A.1) of the second scalar product the identity

$$\| h \|_z = \| F'(z)h \|. \tag{A.5}$$

When we combine (A.4) and (A.5) we obtain from the definition (A.3) of Φ the inequality

$$\Phi(h) \leqslant \| F(z) \|.$$

Next we choose h_S such that

$$F'(z)h_S \equiv F(z) \tag{A.6}$$

which yields from (A.2) the relation

$$\phi'(z)h_S = \| F(z) \|^2.$$

Moreover, due to the special choice (A.6) of h_S we obtain with (A.5)

$$\| h_S \|_z = \| F \|$$

which provides with the definition (A.3) the expression

$$\Phi(h_S) = \| F(z) \|.$$

Consequently the choice of h_S gives the maximizing element for (A.2) and the Newton quotient

$$h_S = (F'(z))^{-1} F(z)$$

following from (A.6) is the required gradient. Thus we realize that the Sobolev gradient of ϕ relative to the natural Riemannian metric is the Newton quotient, thus leading to N in RSN. For complex numbers with $n = 1$ the continuous Newton method gives a flow with respect to the natural Riemannian metric.

With a pedigree like RSN, it should not be a wonder that flows from the continuous Newton method have remarkable properties.

Appendix B. Curl of Newton flow does not vanish in general

In this appendix we calculate with the help of the Cauchy–Riemann differential equations [2] the curl of the Newton flow N of the function F. We present an explicit expression for the curl of N and compare and contrast it to the corresponding equation of electrostatics and magnetostatics.

B.1. Definition of Newton field

We start by defining the components of the Newton flow of a function

$$F(z) = F(x + iy) = u(x, y) + iv(x, y) \tag{B.1}$$

of complex argument $z \equiv x + iy$ and represented by its real and imaginary parts u and v.

From (B.1) and the identity

$$\frac{\mathrm{d}F}{\mathrm{d}z} = \frac{\partial F}{\partial x} = u_x + iv_x,$$

where the subscript x now indicates the partial derivative with respect to x, we find the ratio

$$\frac{F}{F'} = \frac{u + \mathrm{i}v}{u_x + \mathrm{i}v_x} = \frac{(u + \mathrm{i}v)(u_x - \mathrm{i}v_x)}{u_x^2 + v_x^2}$$

or

$$\frac{F}{F'} = \frac{uu_x + vv_x}{u_x^2 + v_x^2} - \mathrm{i}\frac{uv_x - u_x v}{u_x^2 + v_x^2}. \tag{B.2}$$

With the help of the Cauchy–Riemann differential equations

$$u_x = v_y \qquad \text{and} \qquad u_y = -v_x \tag{B.3}$$

we establish the identity

$$uv_x - u_x v = -\left(uu_y + vv_y\right) = -\frac{1}{2}\left(u^2 + v^2\right)_y = -\frac{1}{2}\left(|F|^2\right)_y$$

which together with the relation

$$uu_x + vv_x = \frac{1}{2}\left(u^2 + v^2\right)_x = \frac{1}{2}\left(|F|^2\right)_x$$

reduces (B.2) to

$$\frac{F}{F'} = \frac{1}{2D}\left(|F|^2\right)_x + \mathrm{i}\frac{1}{2D}\left(|F|^2\right)_y,$$

where we have introduced the abbreviation

$$D \equiv u_x^2 + v_x^2 . \tag{B.4}$$

As a result we can identify the individual components

$$N_x \equiv -\,\mathrm{Re}\!\left(\frac{F}{F'}\right) = -\frac{1}{2D}\left(|F|^2\right)_x, \tag{B.5}$$

and

$$N_y \equiv -\,\mathrm{Im}\!\left(\frac{F}{F'}\right) = -\frac{1}{2D}\left(|F|^2\right)_y \tag{B.6}$$

of the Newton field $\boldsymbol{N}$.

B.2. Partial derivatives

We are now in the position to determine the curl

$$\mathrm{curl}\,\boldsymbol{N} \equiv N_{y,x} - N_{x,y}$$

of $\boldsymbol{N}$. Here we have introduced a comma between the two subscripts to separate the components from the variables of differentiation.

From (B.5) and (B.6) we find

$$\mathrm{curl}\,\boldsymbol{N} = -\frac{1}{2}\left[\left(\frac{1}{D}\right)_x\left(|F|^2\right)_y - \left(\frac{1}{D}\right)_y\left(|F|^2\right)_x\right]$$

and when we recall the definition (B.4) of D we obtain

$$\left(\frac{1}{D}\right)_x = -\frac{2}{D^2}(u_x u_{xx} + v_x v_{xx})$$

and similarly

$$\left(\frac{1}{D}\right)_y = -\frac{2}{D^2}\left(u_x u_{xy} + v_x v_{xy}\right).$$

In the last step we have applied the Cauchy–Riemann differential equations (B.3) and the resulting Laplace equation for u and v.

With the help of the relations

$$(|F|^2)_x = 2(uu_x + vv_x)$$

and

$$\left(|F|^2\right)_y = 2\left(uu_y + vv_y\right)$$

we arrive at

$$\text{curl } \boldsymbol{N} = -\frac{2}{D^2}\left\{\left[2u\,u_x v_x + v\left(v_x^2 - u_x^2\right)\right]u_{xx} + \left[-2v\,u_x v_x + u\left(v_x^2 - u_x^2\right)\right]v_{xx}\right\}. \tag{B.7}$$

It is interesting to note, that the curl of $\boldsymbol{N}$ vanishes at points where F or F' vanishes. Moreover, if F is real on the whole real axis, or purely imaginary on the imaginary axis the curl vanishes there [18].

B.3. Summary and comparison to Maxwell field

In the preceding section we have established by a direct calculation for all points z of the complex plane the identity (B.7) which in general is non-vanishing. The deeper reason for this fact can be traced back to the Cauchy–Riemann differential equations discussed above and valid for a holomorphic function

$$\mathcal{F} = \text{Re } \mathcal{F} + \text{i Im } \mathcal{F} = U + iV \ .$$

When we recall that the ratio of two holomorphic functions such as F and F' is also a holomorphic function which implies the Cauchy–Riemann differential equations

$$U_x = V_y \quad \text{and} \quad U_y = -V_x$$

for

$$N = -\frac{F}{F'} = U + iV,$$

the curl of the Newton field reads

$$\text{curl } \boldsymbol{N} = -2V_x. \tag{B.8}$$

A feature common to electrostatics and magnetostatics is the fact that the electric field $\boldsymbol{E} = (E_x, E_y)$ and the magnetic induction $\boldsymbol{B} = (B_x, B_y)$ have a vanishing curl, that is

$$\text{curl } \boldsymbol{E} = E_{y,x} - E_{x,y} = 0$$

and

$$\text{curl } \boldsymbol{B} = B_{y,x} - B_{x,y} = 0.$$

Due to (B.8) in general there is no analogy between the Newton flow and electricity since the curl-free property of the $\boldsymbol{E}$- or $\boldsymbol{B}$-field is violated.

Appendix C. Separatrices

In section 3.2.1 we have used two elementary examples to illustrate the loss of forward uniqueness at a point z_0' where the first derivative F' of F vanishes. We now discuss in more detail the Newton trajectories entering and leaving a simple zero of F'. We conclude by briefly providing an outlook for higher order zeros of F', in particular, we apply our results to the case of a cubic polynomial.

C.1. Simple zero

We start by analyzing the Newton trajectories entering z_0', where $F'(z_0') = 0$ but $F''(z_0') \neq 0$. The Taylor expansion

$$F(z(t)) \cong F(z_0') + \frac{1}{2}F''(z_0')\big[z(t) - z_0'\big]^2 \tag{C.1}$$

of F around z_0' yields

$$z(t) \cong z_0' \pm \left\{\frac{2}{F''(z_0')}\big[F(z(t)) - F(z_0')\big]\right\}^{1/2}.$$

When we recall the solution

$$F(z(t)) = F(z_0')\, \mathrm{e}^{-t}$$

of the differential equation (1) defining the Newton flow, we find

$$z(t) \cong z_0' \pm \left[2\,\frac{F(z_0')}{F''(z_0')}\big(\mathrm{e}^{-t} - 1\big)\right]^{1/2},$$

which reduces for $t \ll 1$ to

$$z(t) \cong z_0' \pm \left[-2\,\frac{F(z_0')}{F''(z_0')}\, t\right]^{1/2}. \tag{C.2}$$

Since $z_0' \equiv z(t = 0)$, there are two trajectories crossing at $t = 0$, that is at the zero of the derivative F'. Hence, negative times close to zero lead to trajectories entering z_0', whereas small positive times correspond to trajectories leaving it.

Moreover, for $t = -|t|$ the trajectories

$$z(-|t|) \cong z_0' \pm \left[\frac{F(z_0')}{F''(z_0')}\right]^{1/2}(2|t|)^{1/2} = z_0' \pm \mathrm{e}^{\mathrm{i}\varphi}\left[2\left|\frac{F(z_0')}{F''(z_0')}\right||t|\right]^{1/2}$$

where

$$\varphi \equiv \frac{1}{2} \arctan \left\{ \frac{\mathrm{Im}\left[F\left(z_0'\right) / F''\left(z_0'\right) \right]}{\mathrm{Re}\left[F\left(z_0'\right) / F''\left(z_0'\right) \right]} \right\}$$

enter z_0' under the angles φ and $\varphi + \pi$. Here we have used the fact that the square root of unity is $\exp\left(\mathrm{i}l2\pi/2\right) = \exp\left(\mathrm{i}l\pi\right)$ with $l = 1$ and $l = 2$, that is -1 and 1.

For $0 < t = |t|$ we obtain from (C.2) with the help of the relation

$$(-1)^{1/2} = \mathrm{e}^{\mathrm{i}\pi/2}$$

the trajectories

$$z(t) \cong z_0' \pm \mathrm{e}^{\mathrm{i}(\varphi + \pi/2)} \left[2 \left| \frac{F\left(z_0'\right)}{F''\left(z_0'\right)} \right| |t| \right]^{1/2}.$$

As a consequence, the trajectories leaving z_0' are orthogonal to the incoming ones.

C.2. Higher order zero

We now turn to a zero of F' of mth order. In this case the Taylor expansion corresponding to (C.1) reads

$$F(z(t)) \cong F\left(z_0'\right) + \frac{1}{m!} F^{(m)}\left(z_0'\right) \left[z_0(t) - z_0' \right]^m$$

where $F^{(m)}$ denotes the mth derivative of F with respect to the argument z of the function F. Thus, we arrive at

$$z(t) \cong z_0' + \left[m! \, \frac{F\left(z_0'\right)}{F^{(m)}\left(z_0'\right)} \, t \right]^{1/m}. \tag{C.3}$$

Since there are m solutions $\exp\left(\mathrm{i}l2\pi/m\right)$ with $1 \leqslant l \leqslant m$ for the mth root of unity we obtain m trajectories entering z_0' and m trajectories that are leaving.

We conclude by illustrating this behavior for the function

$$F_{\mathrm{t}}(z) \equiv z^3 - 1 \tag{C.4}$$

which has the three zeros $\exp\left(\mathrm{i}l2\pi/3\right)$ for $l = 1, 2$ and 3. The origin is a double zero of F_{t}', and (C.3) predicts the three incoming trajectories

$$z_l^{(\mathrm{in})}(t) = z_0' + \exp\left(\mathrm{i}l\frac{2\pi}{3} \right) |t|^{1/3},$$

and the three outgoing trajectories

$$z_l^{(\mathrm{out})}(t) = z_0' + \exp\left(\mathrm{i}l\frac{2\pi}{3} + \mathrm{i}\frac{\pi}{2} \right) |t|^{1/3}.$$

The Newton flow of F_{t} shown in figure 2 confirms these predictions.

Appendix D. Generation of pictures with Mathematica

The pictures of the Newton flow are generated with *Wolfram Mathematica 8* and the commands [3]

$$F[z\_] := ...$$
$$N1[x\_, y\_] := -\text{Re}[F[x + Iy]/F'[x + Iy]]$$
$$N2[x\_, y\_] := -\text{Im}[F[x + Iy]/F'[x + Iy]]$$
$$\text{StreamPlot}\left[\left\{N1\left[x, y\right], N2\left[x, y\right]\right\}, \left\{x, x_0, x_1\right\}, \left\{y, y_0, y_1\right\}\right]$$

The first lines define the function $F(s)$ and the individual components (B.5) and (B.6) of the Newton field N, respectively, whereas the last command produces the Newton flow of F in the intervals $x \in [x_o, x_1]$ and $y \in [y_o, y_1]$. Here, I is the Mathematica code for the imaginary unit i. The zeros, poles and hyperbolic points as well as the separatrices and flow lines on which the function is real are first computed and then indicated by the appropriate symbols.

References

[1] Nunes P 1537 *Treatise in Defense of the Marine Chart*
[2] Whittaker E T and Watson G N 1969 *A Course of Modern Analysis* (Cambridge: Cambridge University Press)
[3] Neuberger J W 1999 Continuous Newton's method for polynomials *Math. Intelligencer* **21** 18
[4] Landau E 1947 Handbuch der Lehre von der verteilung der Primzahlen (New York: Chelsea Publishing)
[5] Maier H and Schleich W P *Prime Numbers 101—A Primer on Number Theory* (New York: Wiley) to be published
[6] du Sautoy M 2003 *The Music of the Primes* (New York: Harper Collins)
[7] Riemann B 1859 Ueber die Anzahl der Primzahlen unter einer gegebenen Grösse *Monatsberichte der Berliner Akadie* Nov. (Translated by D. R. Wilkins, 1998) http://www.claymath.org/publications/riemanns-1859-manuscript
[8] Gourdon X and Demichel P 2004 *The First 10^{13} Zeros of the Riemann Zeta Function, and Zeros Computation at Very Large Height* (http://numbers.computation.free.fr/Constants/Miscellaneous/zetazeros1e13-1e24.pdf)
[9] Odlyzko A M 2001 The 10^{22}-nd zero of the Riemann zeta function *Contemp. Math.* **290** 139
[10] Gutzwiller M C 1991 *Chaos in Classical and Quantum Mechanics* (New York: Springer)
[11] Weidenmüller H A and Mitchell G E 2009 Random matrices and chaos in nuclear physics: nuclear structure *Rev. Mod. Phys.* **81** 539
[12] Weiss C, Page S and Holthaus M 2004 Factorising numbers with a Bose–Einstein condensate *Physica* A **341** 586
[13] Schumayer D and Hutchinson D A W 2011 Physics of the Riemann hypothesis *Rev. Mod. Phys.* **83** 307
[14] Berry M V and Keating J P 1999 The Riemann zeros and eigenvalue asymptotics *SIAM Rev.* **41** 236
[15] Mack R, Dahl J P, Moya-Cessa H, Strunz W T, Walser R and Schleich W P 2010 Riemann ζ function from wave-packet dynamics *Phys. Rev.* A **82** 032119
[16] Twamley J and Milburn G J 2006 The quantum Mellin transform *New J. Phys.* **8** 328
[17] Feiler C and Schleich W P 2013 Entanglement and analytical continuation: an intimate relation told by the Riemann zeta function *New J. Phys.* **15** 063009
[18] Feiler C 2014 Quantum physics and number theory connected by the Riemann zeta function *PhD Thesis* Universität Ulm http:vts.uni-ulm.de/doc.asp?id=8920

[19] van der Pol B 1947 An electro-mechanical investigation of the Riemann zeta function in the critical strip *Bull. Am. Math. Soc.* **53** 976

[20] Berry M V 2012 Riemann zeros in radiation patterns *J. Phys. A: Math. Theor.* **45** 302001

[21] Neuberger J W 2010 *Sobolev Gradients and Differential Equations* 2nd edn (*Lecture Notes in Mathematics* vol 1670) (Heidelberg: Springer)

[22] Lupo D and Payne K R 2000 On the maximum principle for generalized solutions to the Tricomi problem *Commun. Contemp. Math.* **2** 535

[23] van Duzer T and Turner C W 1981 *Principles of Superconductive Devices and Circuits* (New York: Elsevier)

[24] DeGiorgio V and Scully M O 1970 Analogy between the laser threshold region and a second-order phase transition *Phys. Rev.* A **2** 1170

[25] Pitaevskii L and Stringari S 2003 *Bose–Einstein Condensation* (Oxford: Clarendon)

[26] García-Ripoll J J, Konotop V V, Malomed B and Pérez-García V M 2003 A quasi-local Gross–Pitaevskii equation for attractive Bose–Einstein condensates *Math. Comput. Simul.* **62** 21

[27] Neuberger J W 1985 Steepest descent and differential equations *J. Math. Soc. Japan* **37** 187

[28] Neuberger J W 2003 A near minimal hypothesis Nash–Moser Theorem *Int. J. Pure Appl. Math.* **4** 269

[29] Jahnke E and Emde F 1944 *Tables of Higher-Functions with Formulae and Curves* (New York: Dove)

[30] Utzinger A A 1934 Die reellen Züge der Riemann'schen Zetafunktion *Dissertation* Universität Zürich

[31] Speiser A 1935 Geometrisches zur Riemannschen Zetafunktion *Math. Ann.* **110** 514

[32] Arias-de-Reyna J 2003 *X-ray of Riemann zeta function* (arXiv:math/0309433)

[33] Bhaduri R K, Khare A and Law J 1995 Phase of the Riemann ζ function and the inverted harmonic oscillator *Phys. Rev.* E **52** 486

[34] Broughan K A and Barnett A R 2004 The holomorphic flow of the Riemann zeta function *Math. Comput.* **73** 987

Broughan K A and Barnett A R 2007 The holomorphic flow of the Riemann zeta function *Math. Comput.* **76** 2249 (Corrigendum)

[35] Nevanlinna F and Nevanlinna R H 1959 *Absolute Analysis* (Berlin: Springer) (English version 1973)

[36] Sommerfeld A 1988 *Elektrodynamik* (Thun-Frankfurt: Verlag Harri Deutsch)

[37] Neuberger J W 2011 *A Sequence of Problems on Semigroups* (*Problem Books in Mathematics*) (Heidelberg: Springer)

[38] Neuberger J W, Feiler C, Maier H and Schleich W P Newton flow of the Riemann zeta function submitted

[39] Titchmarsh E C 1967 *The Theory of the Riemann Zeta-Function* (Oxford: Clarendon)

[40] Levinson N and Montgomery H L 1974 Zeros of the derivatives of the Riemann zeta-function *Acta Math.* **133** 49

[41] Clay Mathematics Institute *Millenium Prize Problems: Riemann Hypothesis* http://www.claymath.org/millenium-problems/riemann-hypothesis

[42] Karatsuba A A and Voronin S M 1992 *The Riemann Zeta-Function* (Berlin: De Gruyter & Co)

[43] Turán P 1948 On some approximative Dirichlet-polynomials in the theory of the Zeta-function of Riemann *Danske Vid. Selsk. Math.-Fys. Medd.* **24** 36

[44] Montgomery H L 1983 *Studies in Pure Mathematics to the Memory of Pál Turán* ed P Erdös (Basel: Birkhäuser)